ARCH SOC ESP OFTALMOL. 2019;xxx(xx):xxx–xxx

ARCHIVOS DE LA SOCIEDAD ESPAÑOLA DE OFTALMOLOGÍA

www.elsevier.es/oftalmologia

Review

# Update on the usefulness of optical coherence tomography in assessing the iridocorneal angle☆

B. Kudsieh[a,b,*], J.I. Fernández-Vigo[b,c], J. Vila-Arteaga[d,e], J. Aritz Urcola[f,g], J.M. Martínez-de-la-Casa[c], J. García-Feijóo[c], J.M. Ruiz-Moreno[a], J.Á. Fernández-Vigo[b,h]

[a] Departamento de Oftalmología, Hospital Universitario Puerta de Hierro Majadahonda, Madrid, Spain
[b] Centro Internacional de Oftalmología Avanzada, Madrid, Spain
[c] Departamento de Oftalmología, Hospital Clínico San Carlos, Instituto de Investigación Sanitaria (IdISSC), Madrid, Spain
[d] Hospital La Fe, Valencia, Spain
[e] Clínica Vila-Innova Ocular, Valencia, Spain
[f] Departamento de Oftalmología, Hospital Universitario de Álava, Vitoria, Spain
[g] Begitek clínica Oftalmológica. Innova Ocular. Donostia-San Sebastián, Spain
[h] Departamento de Oftalmología, Universidad de Extremadura, Badajoz, Spain

ARTICLE INFO

*Article history:*
Received 17 February 2019
Accepted 20 June 2019
Available online xxx

*Keywords:*
Iridocorneal angle
Optical coherence tomography
Glaucoma
Angle width
Trabecular meshwork
Schlemm's canal

ABSTRACT

The iridocorneal angle, due to its implications in the physiopathology of aqueous humour drainage, is a fundamental structure of the anterior chamber. Anterior segment optical coherence tomography (AS–OCT) is a rapid and non-invasive technique that obtains images in vivo. The high resolution allows it to analyse the normal anatomy of the angle, any alterations, and the changes that occur after different therapeutic interventions. AS–OCT technology has evolved to provide images that allow the identification and quantification of the angular structures in healthy subjects and in glaucoma patients, and especially the trabecular meshwork and the Schlemm's canal. It also enables the angle width to be quantified, with some objective parameters that have been standardised in recent years, such as the trabecular-iris angle (TIA), the angle opening distance (AOD), and the trabecular-iris area (TISA). This technique has multiple uses in the study of the different mechanisms of angle closure, the evaluation of changes after a laser peripheral iridotomy or iridoplasty after cataract surgery, as well as after the implantation of phakic lenses.



☆ Please cite this article as: Kudsieh B, Fernández-Vigo JI, Vila-Arteaga J, Aritz Urcola J, Martínez-de-la-Casa JM, García-Feijóo J, et al. Actualización de la utilidad de la tomografía de coherencia óptica para el estudio del ángulo iridocorneal. Arch Soc Esp Oftalmol. 2019. https://doi.org/10.1016/j.oftal.2019.06.007

* Corresponding author:
E-mail address: bacharkudsieh@gmail.com (B. Kudsieh).

## Actualización de la utilidad de la tomografía de coherencia óptica para el estudio del ángulo iridocorneal

*Palabras clave:*
Ángulo iridocorneal
Tomografía de coherencia óptica
Glaucoma
Abertura angular
Malla trabecular
Canal de Schlemm

RESUMEN

El ángulo iridocorneal por sus implicaciones en la fisiopatología del drenaje del humor acuoso es una estructura fundamental de la cámara anterior. La tomografía de coherencia óptica de segmento anterior (OCT-SA) es una técnica rápida y no invasiva que obtiene imágenes de los tejidos vivos con una alta resolución permitiendo conocer la anatomía normal del ángulo, sus alteraciones y los cambios que se producen en el mismo tras diferentes intervenciones terapéuticas. La tecnología de la OCT-SA ha ido evolucionando hasta ofrecer imágenes que permiten identificar y cuantificar estructuras angulares claves en sujetos sanos y en pacientes con glaucoma, especialmente la malla trabecular y el canal de Schlemm, lo que puede contribuir a ampliar el conocimiento de la fisiopatología del glaucoma. Además, permite cuantificar la abertura angular con unos parámetros objetivos descritos en los últimos años, entre los que destacan el ángulo irido-trabecular (TIA), la distancia de abertura angular (AOD) y el área irido-trabecular (TISA). La OCT-SA presenta múltiples utilidades en el estudio de los distintos mecanismos del cierre angular, la evaluación de los cambios angulares tras la realización de una iridotomía láser o iridoplastia, cirugía de la catarata o el implante de lentes fáquicas.



## Introduction

Due to its implications in the physiopathology of aqueous humor (AH) drainage, the iridocorneal angle is a fundamental structure in the anterior chamber of the ocular globe. In recent years, the development of anterior segment optical coherence tomography (AS–OCT), an imaging technique based on low coherence interferometry that obtains in real time a fast and noninvasive examination providing images of life tissue with high resolution, has enabled extremely detailed iridocorneal angle assessments. OCT technology developments in capture speed and image resolution has allowed this technology to become an essential examination tool in ophthalmological practices.[1–12]

Different OCT devices enable the assessment of the angular region (Table 1). Some of the main advantages of AS–OCT include the possibility of identifying the structures that comprise the angle, objectively measuring the angle region, exploring the angle in pediatric patients or those exhibiting traumatism because it is a noncontact examination which does not require anesthesia. In this way, the angle can be assessed even in the presence of angular opacities.[1,2]

In addition, OCT technology exhibits excellent reproducibility (intraclass correlation coefficient of >0.9) for measuring angle parameters utilizing different devices.[3,4] However, even though various studies have found a good match between angle measures obtained with different OCT devices,[5] absolute values are not interchangeable.[6]

### *Evaluation of iridocorneal angle structures with AS–OCT*

In recent years, several authors have described the ways in which AS–OCT facilitates the identification of angle region structures as well as AH drainage pathways (Fig. 1).

*Trabecular meshwork (TM):* due to its relevance in AH drainage, one of the main analyzed structures was TM. In 2008, Sarunic et al. obtained the first image thereof.[7] TM is identified as the hyper-refringent half-moon in the scleral groove, anteriorly limited by Schwalbe's line and posteriorly by the scleral spur. Its identification varies between authors (Table 2), with the high resolution images provided by said technology enabling the assessment of its dimensions. Utilizing Swept source AS–OCT, Tun et al.[11] obtained a mean TM length of $779 \pm 98\,\mu m$, although it must be said that they did not directly visualize the TM and therefore their measurements were indirect from the scleral spur up to Schwalbe's line. In their study on TM with a sample of 1006 healthy Caucasian individuals, Fernández-Vigo et al.[10] observed a mean length of $497 \pm 93\,\mu m$, a thickness of $174 \pm 28\,\mu m$ and an area of $0.069 \pm 0.031\,mm^2$. Other authors such as Cheung et al.[12] and Usui et al.[13] found similar TM measurements, with a mean length of $467 \pm 60\,\mu m$ and $467 \pm 61\,\mu m$, respectively. The latter authors observed a mean area of $0.067 \pm 0.058\,mm^2$. The aforementioned study by Fernández-Vigo et al.[10] showed TM as an independent structure from the rest of studied parameters and did not observe association between TM size with age, axial length, anterior depth chamber or with angle opening.

*Schlemm's canal (SC):* in OCT, the SC is seen as a long and narrow hypo-reflective space outside of the TM. Kagemann et al.[14] were the first to identify it through OCT (Table 2). Due to the high resolution of the latest OCT devices, at present it is possible not only to identify but also quantify SC size after several procedures. A study carried out by the authors' group on the SC measurements in a population of healthy children[15] found a similar SC diameter in the temporal and nasal quadrants of $267 \pm 84\,\mu m$ (range 131–509) and $273 \pm 77\,\mu m$ (range 124–486), respectively ($p = 0.125$). The SC area was also similar between both quadrants, $9.975 \pm 3.514\,\mu m^2$ (range 4.000–23.000) versus

**Table 1 – Characteristics of the main optical coherence tomography devices.**

| OCT model | Manufacturer | Optical source | Axial resolution[a] | Transversal resolution[a] | Scan rate A-scans/second | Scan depth | Maximum scan width |
|---|---|---|---|---|---|---|---|
| Visante | Carl Zeiss Meditec, Dublin, AC | SLD 1310 nm | 18 μm | 60 μm | 2000 | 6 mm | 16 mm |
| Slit Lamp | Heidelberg Engineering, Heidelberg, Germany | SLD 1310 nm | <25 μm | 20-100 μm | 200 | 7 mm | 15 mm |
| Optovue RTVue | Optovue, Inc, Fermont, AC | SLD 840 nm | 5 μm | 15 μm | 26,000 | 2 mm | 6 mm |
| Spectralis | Heidelberg Engineering, Heidelberg, Germany | SLD 820 nm | 7 μm | 20 μm | 40,000 | 2 mm | 6 mm |
| Cirrus | Carl Zeiss Meditec, Dublin, AC | SLD 840 nm | 5 μm | 15 μm | 27,000 | 2 mm | 6 mm |
| Casia SS-1000 | Tomey Corporation, Nagoya, Japan | SS láser 1310 nm | 10 μm | 30 μm | 53,000 | 2 mm | 8 mm |
| Nidek RS 3000 | Nidek, Gamagori, Japan | SLD 880 nm | 7 μm | 15 μm | 100,000 | 6 mm | 12 mm |
| Triton | Topcon Corporation, Tokyo, Japan | SS láser 1310 nm | 8 μm | 30 μm | 30,000 | 6 mm | 16 mm |

OCT: optical coherence tomography; SLD: Super Luminescent Diode; SS: Swept Source.

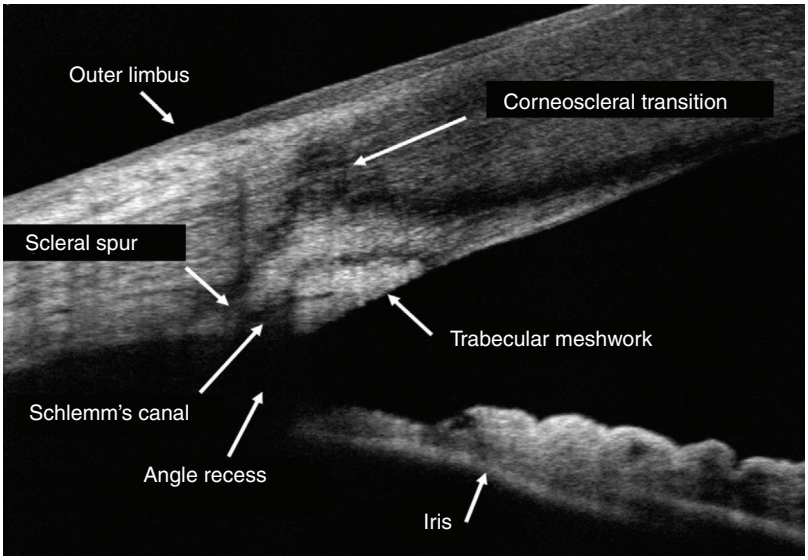


**Fig. 1 – Identification angle region structures with optical coherence tomography.**

**Table 2 – Identification percentage of angle structures with anterior segment optical coherence tomography.**

| Angle structure | Identification percentage | Subjects | OCT | Authors, year |
|---|---|---|---|---|
| Schwalbe's line | 95% | 73 healthy | Cirrus | Cheung et al.[12] |
| Trabecular meshwork | 82% | 69 healthy | Cirrus | Quek et al.[8] |
| | 62.2% | 45 healthy | Cirrus | Wong et al.[9] |
| | 91% | 1006 healthy | RTVue | Fernández-Vigo et al.[10] |
| Schlemm's canal | 100% | 10 healthy | Cirrus | Kagemann et al.[14] |
| | 70% | 290 healthy children | RTVue | Fernández-Vigo et al.[15] |
| | 80% | 50 OAPG | RTVue | Hong et al.[17] |
| | 86% | 50 healthy | | |
| | 87,7% | 41 healthy | RTVue | Imamoglu et al.[18] |
| | 70.7% | 41 PSX | | |
| Scleral spur | 100% | 60 healthy | CASIA | Usui et al.[13] |
| | 88% | 265 healthy | RTVue | Grewal et al.[32] |
| | 78% | 45 healthy | Cirrus | Wong et al.[9] |

OAPG: open angle primary glaucoma; PSX: pseudoexfoliation.

$9.688 \pm 3.297\,\mu m^2$ (range 3.000–24.000) ($p = 0.167$). No differences were observed in SC size per sex, refractive defect or TM size ($R \leq 0.116$; $p \geq 0.125$). However, said study did observe larger SC size with the increase of age in children ($p = 0.041$). Chen et al.[16] obtained a mean SC area in healthy adults of $2.759 \pm 823\,\mu m^2$ and $2.909 \pm 827\,\mu m^2$ for the nasal and temporal sectors, respectively. Hong et al.[17] observed smaller SC sizes in patients with open angle primary glaucoma (OAPG) when compared to healthy subjects ($11{,}332 \pm 2015\,\mu m^2$ vs. $13.991 \pm 1.357\,\mu m^2$; $p < 0.001$). In turn, Imamoglu et al.[18] also observed smaller SC sizes in patients with pseudoexfoliative glaucoma than in healthy subjects ($4000\,\mu m^2$ vs. $5000\,\mu m^2$; $p = 0.036$).

The differences between absolute values of SC size observed by several authors in healthy populations must be noted. This could be due to the use of different OCT devices. In what concerns intraocular pressure (IOP), Hong et al.[17] did not find a correlation with SC area. However, a correlation has been found between IOP reduction after medical or surgical glaucoma treatment and SC size increases. Accordingly, Chen et al.[16] observed a 90% increase in SC size after instilling travoprost, while Skaat et al.[19] documented a 21% increase in SC area in healthy subjects and 24% SC increase in patients with OAPG after instilling pilocarpine. In addition, it has been observed that other procedures could induce changes in SC size. Thus, Zhao et al.[20] observed a sustained dilatation of SC during the first 6 months after phacoemulsification. Skaat et al.[21] described an 8% increase in SC area after selective trabeculoplasty. SC size changes have also been described after a range of surgeries such as trabeculectomy ($5200 \pm 996\,\mu m^2$ pre-surgery vs. $8117 \pm 1942\,\mu m^2$ post-surgery; $p < 0.001$)[22] or canaloplasty (SC heights and weights increased 369% and 152%, respectively).[23]

Recently, Huang et al.[24] carried out a very interesting line of research, describing AH angiography in order to obtain in-depth knowledge of its drainage pathways, observing sectorial, pulsating and dynamic patterns. Said authors utilized AS–OCT for interpreting this new research to identify the intra-scleral spaces represented by the collectors that are part of the drainage pathways with the objective of optimizing the surgical results of various glaucoma techniques.

*Scleral spur:* it can be observed as a hyper-reflective area in the posterior vertex of TM, forming part of the angle recess. The percentage of identification is generally high in most studies (>70%) (Table 2). Scleral spur identification is of vital importance for OCT involving automatic angle analysis software because it is the reference point for taking several measurements. For this reason, interobserver variability in the identification of the scleral spur could give rise to differences in the classification of open and closed angles.[25]

### Correlation with other angle assessment techniques

*Gonioscopy:* the reference examination for angle assessment. However, it comprises several drawbacks due to being a subjective technique requiring an expert examiner in addition to being uncomfortable for patients and the fact that it does not provide quantitative data, all of which limits its usefulness. The advantages of gonioscopy compared to OCT include direct visualization of angle structures, particularly the TM and its pigmentation degree, dynamic angle evaluation to differentiate apositional from synechial angle closure and the visualization of blood in CS.[26] The match between AS–OCT and gonioscopy to detect angle closure ranges between moderate and good both in healthy subjects and in glaucomatous patients (sensitivity: 73–95% and specificity: 59–84%).[27–29] In a study comprising 423 eyes, Sakata et al.[30] found that AS–OCT overestimates angle closure when compared to gonioscopy. In addition, they observed that in the presence of discrepancies between both techniques, AS–OCT tends to classify temporal quadrants as being more open than in gonioscopy. However, in the lower and upper quadrants, gonioscopy tends to classify angles as open whereas AS–OCT classifies them as closed.

*Devices based on the Scheimpflug camera*: these devices comprise a rotational camera that captures 50 meridional images in under 2 s, and is able to produce 3 D images and enabling angle opening quantification. In a previous paper studying angle opening measurement matches between the Scheimpflug camera and OCT carried out by the authors' group, a total CCI of 0.378 and 0.589 was obtained for the temporal and nasal sectors, respectively, producing a match between low and moderate.[31] In comparison to OCT, the Scheimpflug camera tends to overestimate opening in narrow angles and underestimate opening in open angles. Interestingly, Grewal et al.[32] observed that the parameter obtained with the Scheimpflug camera that best correlated with angle opening assessed with OCT or gonioscopy was anterior chamber volume.

*Ultrasound biomicroscopy (UBM):* this is an ecographic technique that utilizes high-frequency ultrasound transducers (50–100 MHz) and has become the reference for studying the posterior chamber and retro-iridian structures. The usefulness of UBM for assessing the angle region includes iris configuration analysis and ciliary body arrangement, cystic angle closure, study of lenses in sulcus, plateau iris as well as for the differential diagnostic of ciliary, angle or iris tumors. Mansouri et al.[33] carried out a comparative study observing that the AS–OCT measurements exhibited good overall correlation with those taken by means of UBM for evaluation of angle opening. Even so, said authors frequently observed significant differences in the measurements between both devices.

### Quantitative parameters of angle study with AS–OCT

In recent years, a number of parameters have been standardized for measuring angle opening, as described in Table 3.

*Angle opening* (measured in degrees; trabecular-iris angle [TIA]; or anterior chamber angle [ACA]): (Fig. 2). TIA was described in 2005 by Radhakrishnan et al.[34] who carried out a study to classify potentially occludable angles comparing OCT with Ernie Oscar B and UBM. In a population of 989 subjects, Fernández-Vigo et al.[4] were able to measure TIA in 94% of cases with OCT RTVue, obtaining a mean value of $35.8 \pm 13.2$ degrees. In addition, said authors observed a correlation between refractive defect and TIA, with angle opening remaining stable between −9 and −3 diopters (D) with a mean angle of 46°. With the development of −3D, the angle narrowed 2.7° for every D of positive increase, reaching an angle open-

**Table 3 – Parameters utilized in angle region measurements with optical coherence tomography (OCT).**

| Parameter | Definition |
|---|---|
| Angle opening (in degrees) or trabecular iris angle (TIA) | Obtained starting from angle recess and locating one of the lines at the trabecular meshwork starting point (in the area close to Schwalbe's line) and locating the other line over the iris surface reaching the perpendicular point that crosses with the trabecular meshwork line (Fig. 2) |
| Angle opening distance (AOD) | Obtained drawing a line from the scleral spur towards the corneal endothelium at 500 ($AOD_{500}$) or 750 microns ($AOD_{750}$) followed by another line from said corneal endothelium point perpendicular thereto up to the surface of the iris. The most utilized parameter for angle assessment is $AOD_{500,}$ with $AOD_{750}$ being more useful to study iris conflagration so that if $AOD_{750}$ is lower than $AOD_{500}$ its means that angle tends to narrow instead of increasing. (Fig. 3A) |
| Iris-trabecular area (TISA) | Trapezoidal area comprise between the AOD, the surface of the iris, the corneal endothelium and a right angle line starting from the scleral spur towards the iris. This area does not include the angle recess area (posterior to the scleral spur) because in theory it is regarded as a non-filtrating area. (Fig. 3A) |
| Trabecular - iris contact length (TICL) | Linear distance of contact between the iris and the trabecular meshwork from the scleral spur. Only measurable in closed angles because said contact exists only under said condition (Fig. 5) |
| Iridian thickness (IT) | Drawing a line from the scleral spur towards the corneal endothelium at 500 or 750 microns and subsequently another line from said point of the corneal endothelium at right angles up to the surface of the iris. The shortest distance between these points in the anterior surface of the iris to the posterior surface thereof is calculated as $IT_{500}$ and $IT_{750}$ |
| Iris curvature (IC) | Perpendicular distance from the posterior/anterior surface of the iris at the point of greatest complexity/concavity up to a line between the root of the iris up to the most peripheral point of the iris pigment epithelium |

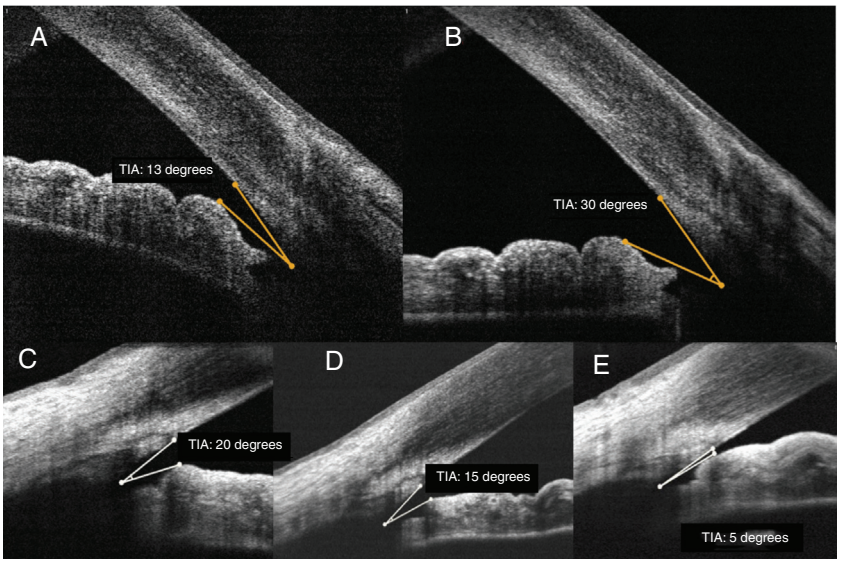


**Fig. 2 – Assessment of angle opening with optical coherence tomography pre- A) and post- B) cataract surgery, showing how angle opening increases after surgery. Presurgery image C), post-surgery month 1 D) and one year E) of a phakic epi-crystalline lens in a hypermetropic patient. Diminished angle opening can be observed.**

ing of only 20° in hypermetropic patients (>7D). Similarly, it was observed that the angle narrowed with age at a rate of 0.57 degrees per year as of age 18 (mean angle: 50 degrees) up to age 60 (mean angle: 30 degrees), remaining subsequently stable. In addition, said study observed that the anterior chamber (AC) volume followed by AC depth constitutes the ocular parameters that best correlated with TIA ($R > 0.80$; $p < 0.001$). Also, lower mean angle opening was observed in females (4.5 degrees, $p < 0.001$). Similarly, in the Beijing Eye Study carried out on an Asian population of 2985 healthy subjects, Xu et al.[35] observed with AS–OCT utilizing OCT Visante a mean TIA of $38 \pm 16$ degrees, with smaller angle opening being associated to females, hypermetropia, higher age and less central corneal thickness.

*Angle opening distance* (AOD), introduced by Pavlin et al.[36] utilizing UBM to quantify angle opening (Fig. 3A; Table 3). The most widely used is $AOD_{500,}$ With $AOD_{750}$ being more useful for studying iris configuration. It has been observed that AOD values vary according to race and measuring device. Thus, in a healthy Asian population Leung et al.[37] found $AOD_{500} = 527 \pm 249\,\mu m$ with OCT Visante, a reading similar to that observed by Fernandez-Vigo et al.[4] who found with

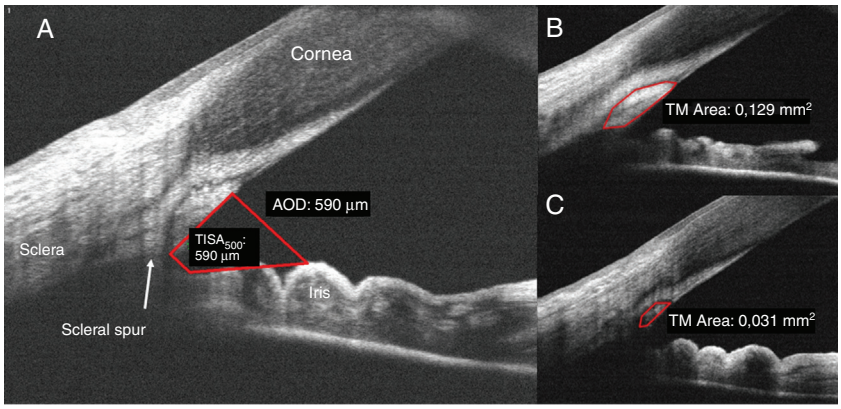


**Fig. 3 – A) angle region measurements with optical coherence tomography applying new standardized parameters. AOD: angle opening distance and TISA: trabecular-iris area measured at 500 µm from the scleral spur. B and C) different trabecular meshwork sizes.**

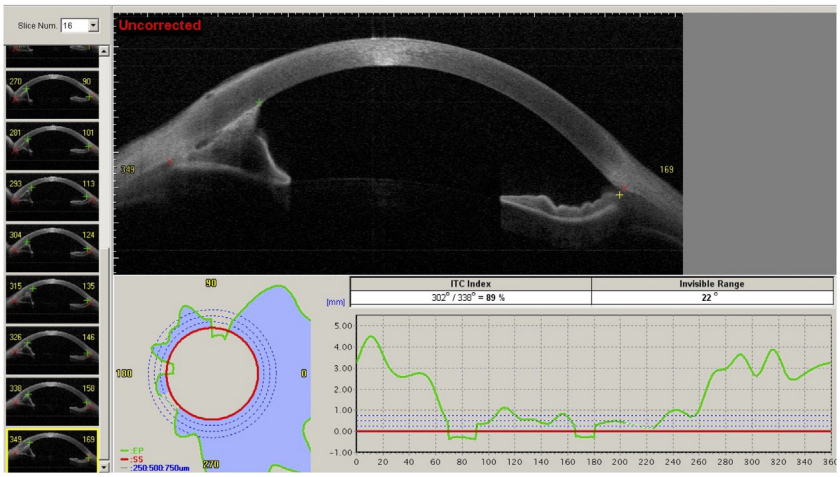


**Fig. 4 – Índice Trabecular-iris contact index (TIC). For calculating the TIC index the scleral spur must be located together with the contact points between the iris and the trabecular meshwork-endothelium within 360° of the anterior chamber. This indicates the trabecular meshwork percentages obstructed by iris tissue.**

Fourier domain OCT RTVue an $AOD_{500}$ = 537 ± 292 µm in a Caucasian population, whereas in patients with angle closure Mansouri et al.[33] found a markedly diminished AOD ($AOD_{500}$ = 210 ± 16 µm).

In what concerns the correlation between $AOD_{500}$ measured with Slit-lamp OCT and gonioscopy, Wirbelauer et al. found a good correlation (R = 0.80) between gonioscopy and AOD to classify narrow angles (Shaffer ≤2 in all quadrants, sensitivity 85% and 90% specificity).[38] Concerning the usefulness of this parameter in daily clinic practice, Radhakrishnan et al.[34] and Cheung et al.[12] suggested $AOD_{500}$ values ≤191 and 172 µm, respectively, in order to detect occludable angles (Shaffer ≤1) to establish indication for peripheral laser iridotomy (PLI).

*Trabecular-iris space area [TISA]*: this parameter was also first described by Radhakrishnan et al.[34] TISA would represent the effective filtering area of TM as it excludes the non-filtrating region behind the scleral spur or angular recess (where TM no longer exists; Table 3). As with AOD, TISA can be measured and 500 or 750 µm from the scleral spur (Fig. 3A). A mean $TISA_{500}$ of 0.193 ± 0.102 $mm^2$ by means of OCT- Visante was found in the Leung et al. study,[37] whereas said parameter was 0.195 ± 0.103 $mm^2$ in the Fernández-Vigo et al. study with RTVue.[4] Even though TISA is a parameter that was proposed to represent the effective filtering area of TM, a range of population studies have not found a correlation with IOP.[35]

*Index of trabecular-iris contact [TIC]*: this term was introduced after a semiautomatic analysis with the CASIA device (Tomey Corporation, Nagoya, Japan) that assessed the percentage of 360-degree trabecular-iris contact (Fig. 4). A study on an Asian population by Baskaran et al.[39] observed that eyes with open angle in gonioscopy produced a TIC of 15.2%, with 48.5% in eyes with closed angle. Said authors concluded that if TIC >35% sensitivity and specificity for detecting angle closure was 71.9% and 84.3%, respectively.

*Trabecular iris contact length [TICL]*: by virtue of the high-resolution provided by the latest OCT devices, this new parameter was proposed to represent the linear contact distance between the iris and the TM (Fig. 5), with the ability to precisely quantify said contact. In a healthy population

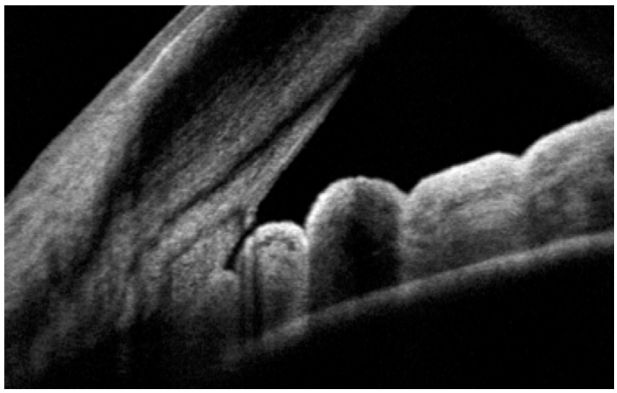

**Fig. 5 – Length of iris-trabecular contact (TICL: trabecular iris contact lentgh).**

comprising 2012 eyes, Fernández-Vigo et al.[40] observed a trabecular iris contact length of 1.6%, with the mean TICL in said patients being 239 ± 79 μm over a mean TM size of 486 ± 86 μm. Said trabecular iris contact was only observed in angles <23 degrees, with a weak correlation between TICL and IOP (R = 0.270). In addition, due to the high-resolution provided by the latest OCT devices, Fernández-Vigo et al. proposed measuring the TICL percentage, i.e., the percentage of TM occluded by the iris which in their study reached 46.9 ± 13.9% (range 17.2–76.3%). A very interesting study was published by Chong et al. on a population of 2045 subjects reporting an association between angle closure degree (assessed with gonioscopy and OCT) and IOP, although it should be noted that IOP increase was slight (no closed quadrant: 14.7 ± 0.2; one quadrant: 15.0 ± 0.2; two: 14.8 ± 0.2; three: 15.1 ± 0.3;four : 16.0 ± 0.3 mm Hg; P < 0.001).[41]

### *Clinic usefulness of iris-corneal angle assessment with AS–OCT*

Angular assessments with OCT include numerous useful purposes (Table 3):

*Angle closure mechanisms:* Shabana et al.[42] carried out a study to assess the primary angle closure mechanisms (including pupil blockage, plateau iris, increased lens vault and the role of thick and peripheral iris) analyzing angle parameters with AS–OCT. said authors found higher.

$AOD_{500}$ and $AOD_{750}$ values in the plateau iris group (0.09 ± 0.02 mm and 0.19 ± 0.02 mm, respectively) due to the fact that in this case angle opening was not diminished. Likewise, Guzman et al.[43] used angle parameters obtained with AS–OCT to differentiate between suspected angle closure, factual angle closure and glaucoma due to angle closure in 425 subjects. The highest $AOD_{750}$ values were exhibited by the suspected angle closure group (0.28 ± 0.007 mm) followed by the factual angle closure and the glaucoma due to angle closure groups, respectively (0.24 ± 0.012 mm and 0.23 ± 0.009 mm; p < 0.001).

In what concerns secondary angle closure mechanisms, AS–OCT can also play a crucial role for diagnosis, classification and follow-up of evolution (Fig. 6). Kwon et al.[44] divided eyes with primary angle closure in 2 subgroups on the basis of the characteristics observed with OCT and UBM, reporting that angle opening was a main difference in said subdivision, with the ciliary body position being another important factor. They also observed that both factors had a repercussion in pressure decrease after PLI (Fig. 7).

*Malign glaucoma:* Wirbelauer et al.[45] carried out the first study assessing the usefulness of angle OCT for malign glaucoma after filtrating surgery, reporting 2 cases in which, after performing vitrectomy, TIA and $AOD_{500}$ increased from 0, in both cases to 35 degrees and 425 μm, respectively.

*Neovascular glaucoma:* OCT was also used in neovascular glaucoma for identifying the hypo-reflectiveness tissue in the angle corresponding to neovessels as well as to assess the regression thereof after antiangiogenic therapy.[46] By means of OCT, Nadal et al. observed that antiangiogenic monotherapy is frequently not enough to eliminate fibrovascular tissue and could induce the contraction thereof thus worsening angle closure.[47]

*Pigment dispersion syndrome and glaucoma:* AS–OCT can also be utilized in the diagnostic and follow-up of the pigment dispersion syndrome (PDS), characterized by a broad iris-cornea angle due to the concavity of the peripheral iris, giving rise to inverted pupil blockage and mechanical friction of the iris against the lens surface (Fig. 8A), with the ensuing release of pigment. In a study on 63 eyes with PDS and pigment glaucoma, Bimer et al.[48] observed that the parameters measuring angle opening were larger in these patients (grouping PDS and pigment glaucoma) than in controls ($AOD_{500}$ = 0.782 ± 0.304 mm vs. 0.561 ± 0.252 mm; $AOD_{750}$ 1.028 ± 0.364 mm vs. 0.729 ± 0.241 mm; $TISA_{500}$ 0.288 ± 0.120 $mm^2$ vs. 0.201 ± 0.083 $mm^2$; p < 0.001). An interesting study carried out by Aptel et al.[49] using OCT reported to diminished contact between iris and lens in PDS after peripheral laser iridotomy (PLI) (0.42 $mm^2$ vs. 0.11 $mm^2$; p < 0.001), with values after IPL being similar to those of the control group (Fig. 8B).

*Pseudoexfoliation syndrome:* OCT has also been utilized in subjects with the pseudoexfoliation syndrome (PSX) in a study by Fernández-Vigo et al.[50] that did not find differences in angle opening vis-à-vis healthy controls. OCT enabled the assessment of sedimentation in the lens anterior surface and the endothelium, although no identifiable PSX sedimentation was observed in the iris-cornea angle.

It is worthwhile noting that in recent years the use of OCT has become widespread for assessing changes that take place in the angle after different ocular interventions through laser or surgical techniques in order to understand changes on the AH drainage system in an attempt to predict its effects on IOP (Table 4).

*Laser iridotomy or iridoplasty:* several studies have demonstrated the possibility of objectively observing and quantifying increases in angle parameters (TIA, AOD and TISA) obtained with AS–OCT after PLI or iridoplasty in the presence of angle closure.[51,52] After performing PLI in eyes under the effects of an acute glaucoma episode as well as in the contralateral eye, Moghimi et al. (Fig. 9A and C), observed increases in $AOD_{500}$ (150 ± 24 μm a 550 ± 61 μm) in eyes under said episode as well as in contralateral eyes (350 ± 38 μm a 770 ± 60 μm).[51] In order to predict the success factors of PLI in patients with suspected angle closure, Lee et al.[53] found that lower pretreatment val-

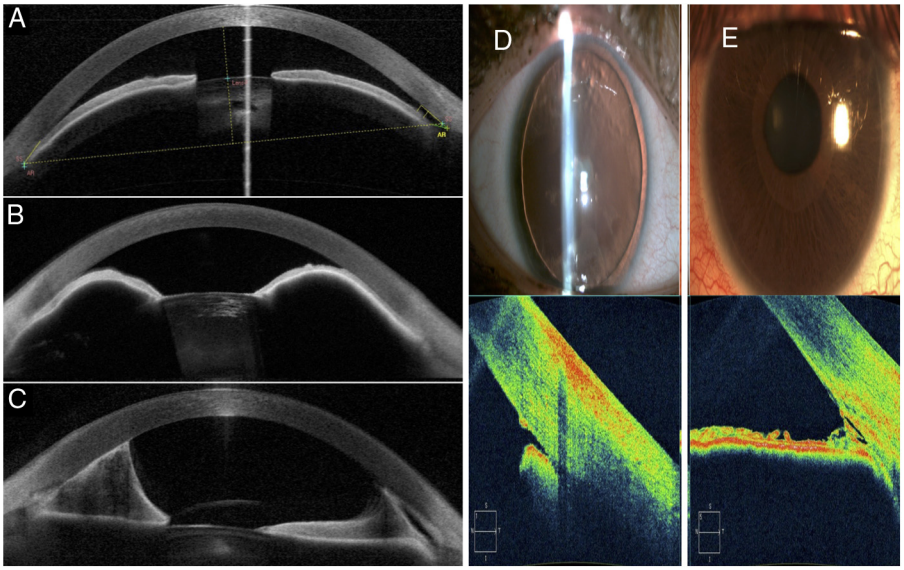


**Fig. 6 – Anterior segment optical coherence tomography (AS–OCT) with secondary angle closure due to several mechanisms. A) phakomorphic glaucoma. B) anteriorly protruded iris. C) anterior synechiae. D) Aniridia. E) Axenfeld-Rieger syndrome. (E: courtesy of Dr. Santos Bueso).**

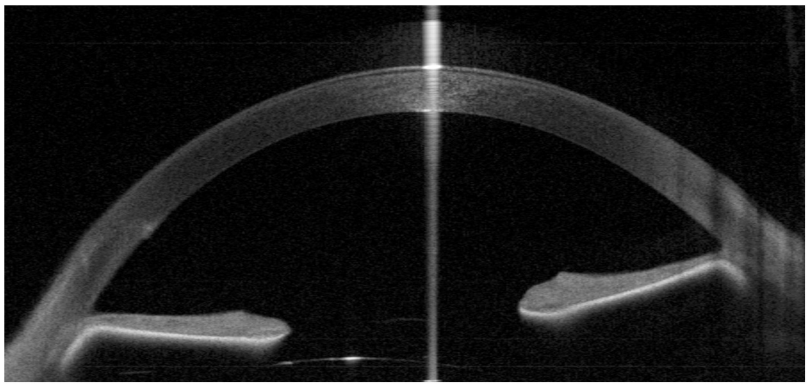

**Fig. 7 – Neovascular glaucoma showing 360° synechiae with iris rectification by means of optical coherence tomography.**

**Table 4 – Usefulness of iridocorneal angle examination with optical coherence tomography (OCT).**

| Parameter | Definition |
|---|---|
| Identification of structures | Measurement of trabecular meshwork size and Schlemm's canal |
| Assessment of angle opening modifications | After laser interventions (iridotomy and iridoplasty), cataract surgery, phakic lens implant surgery, after glaucoma surgery |
| Assessment of angle closure | Study of the mechanism that accounts for primary and secondary angle closure, quantification of iris-trabecular contact, assessment and follow-up of synechiae |
| Assessment of secondary glaucomas | Pigment dispersion: iris concavity and friction over the lens before and after iridotomy<br>Neovascular glaucoma: angle classification, the progression or regression of synechial angle closure after treatment.<br>Malign glaucoma: assessment of angle closure mechanisms after filtrating surgery |
| Pediatric patients and traumatisms | Evaluation angle alterations in congenital glaucoma, angle recession after traumatism, cysts and angle-iris tumors |

ues of TIA, AOD and TISA were associated to larger short-term angle opening after PLI (2–3 weeks). Similarly, Sung et al.[54] found that eyes with baseline values under $AOD_{750}$ and $IT_{750}$ exhibited larger changes in angle opening both in the short-term (2 weeks) and in the longer term (3 years) after PLI. In addition, Ang et al. found that PLI is more likely to fail in the presence of higher TICL and lower iris anterior curvature.[55]

*Cataract surgery:* regarding angle changes after lens surgery (Fig. 2. 9 B and D), Zhou et al.[56] studied the presurgery TIA values obtained with AS-OCT Visante as a predictive factor

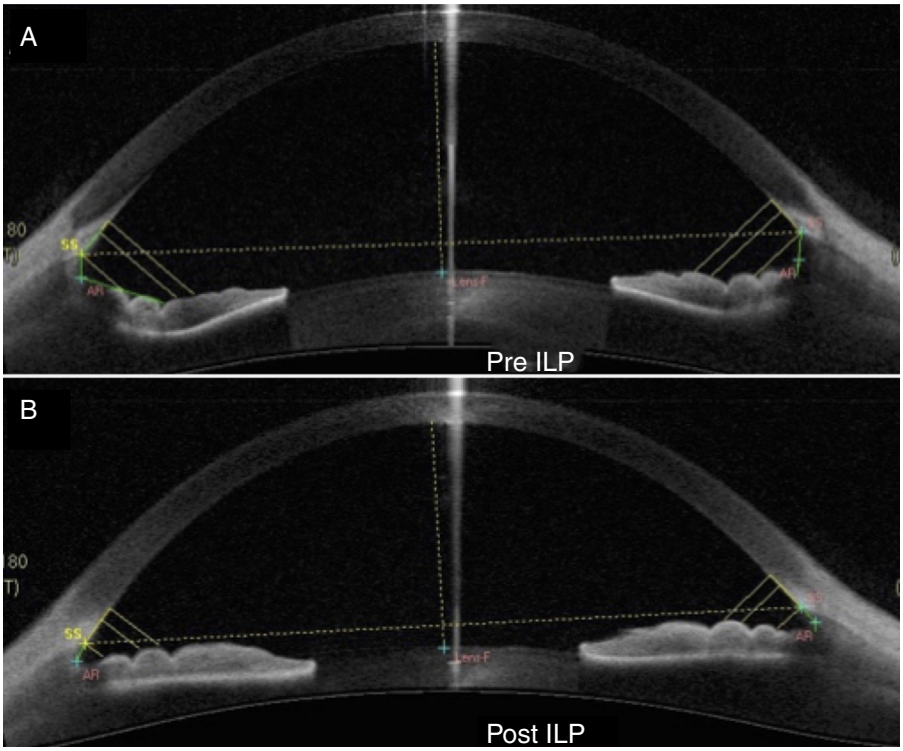


**Fig. 8 – Evolution control in pigment dispersion syndrome pre- A) and post- B) treatments by means of peripheral laser iridotomy (PLI).**

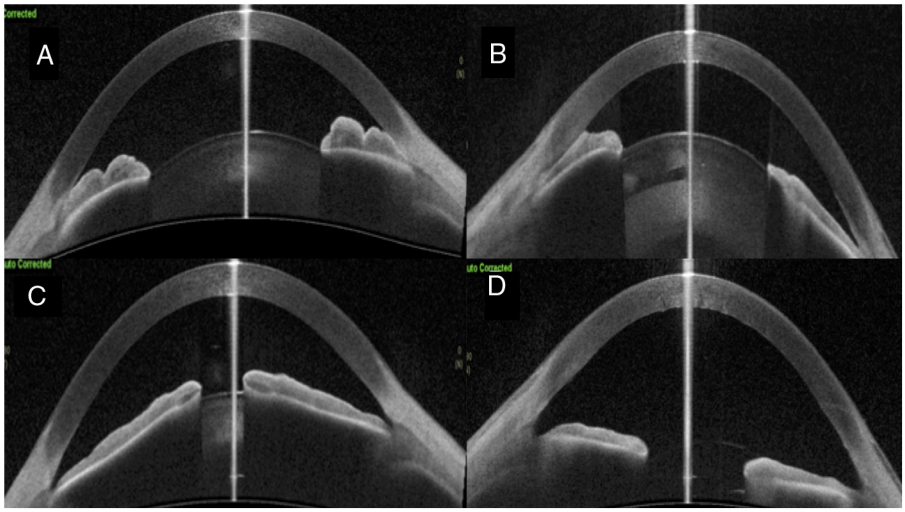


**Fig. 9 – Evaluation with optical coherence tomography of angle opening in 2 clinic cases. Case A) exhibits pupil blockage with intraocular pressure (IOP) of 36 mmHg, resolved after YAG iridotomy with IOP normalization to 18 mmHg, image C). Angle opening can be seen increased. Case B) exhibits an acute glaucoma episode with goniosynechiae, showing a resolution of the condition D) after cataract surgery and goniosynechiolysis.**

for post-surgery IOP changes and observed that the angle increased (TIA from 25 to 38 degrees) and and that mean IOP diminished from 15.1 to 12.8 mm Hg. However, said authors concluded that the preop angle measurements were unable to predict the hypotensor effect of IOP after cataract surgery. Similarly, Huang et al.[57] assessed the predictive capacity of several parameters ($AOD_{500}$, $TISA_{500}$, TIA, lens vault and iris curvature) on IOP reduction after cataract surgery in eyes without glaucoma, including patients with narrow and open angle. Accordingly, both the lens vault and increased $AOD_{500}$ after surgery ($R = 0.240$. $P = 0.041$) exhibited a correlation with IOP reduction ($R = 0.235$; $P = 0.045$; $14.97 \pm 3.35$ to $12.62 \pm 3.37$ mm Hg; $p < 0.001$). In agreement with the previous study, Hsia et al. found in a multivariable analysis that in presurgery IOP

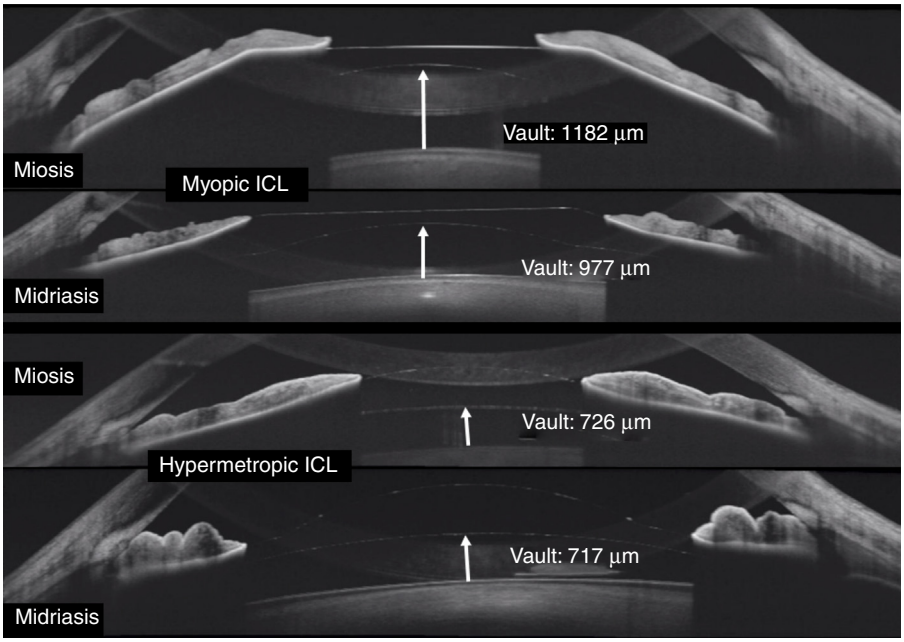


**Fig. 10 – optical coherence tomography images showing the position of the myopic and hypermetropic ICL lens in miosis and midriasis, with the possibility of assessing secondary angle changes.**

($R^2 = 0.40$; $p < 0.001$), $AOD_{500}$ ($R^2 = 0.45$; $p = 0.02$) and lens vault ($R^2 = 0.47$; $P = 0.009$) were able to predict IOP reduction after cataract surgery in patients with OAPG.[58]

*Phakic lenses:* AS–OCT has also demonstrated its usefulness for angle assessment after implanting phakic lenses for correction of various refractive defects (Fig. 10). Fernández-Vigo et al.[59] observed that angle opening diminished 34–42% one month after implanting a myopic epicrystalline lens (ICL V4c, STAAR Surgical AG), and also observed a significant AOD reduction one month after surgery ($804.6 \pm 276.8$ μm to $3694 \pm 1699$ μm; $p < 0.001$). However, the 2-year follow-up of these patients evidenced angle closure stabilization (AOD at month 369 was ±170 vs. $354 \pm 152$ at 2 years; $p = 1{,}0$).[60] TIA correlated with the lens vault 2 years after surgery ($R = -0.609$; $p < 0.001$). In addition, iris-trabecular contact was observed in 8 of the 54 studied eyes in the first month after ICL implant which did not progress at 2 years after said implant. In these cases, mean TICL was $307 \pm 288$ μm. Interestingly, 7 presurgery factors were identified that could predict angle opening after ICL implant (TIA, age, sex, refractive defect, $IT_{500,}$ white to white distance and lens size) with $R^2 =$ of 0.915. 0.839 and 0.805 for the temporal, nasal and inferior sectors, respectively ($P < 0.001$). Factors such as anterior chamber depth, axial length or lens power were found to be not determining ($p \geq 0.05$). As in the study of Fernández-Vigo et al., Yan et al.[61] did not find either that reductions in TIA, AOD and TISA after ICL implants correlated with increased IOP during 2 years after the ICL implant.

## Conclusions

AS–OCT technology has evolved in recent years to provide images enabling the identification and quantification of key angle structures to determine normal angle anatomy and its alterations. This could contribute to increase our knowledge on the physiopathology of glaucoma.

Said technology enables the quantification of angle opening with objective parameters, mainly trabecular-iris angle (TIA), angle opening distance (AOD) and trabecular-iris surface (TISA). In addition, OCT comprises a broad range of functions for studying angle closure mechanisms, assessing changes after laser iridotomy or iridoplasty cataract surgery or implant of phakic lenses.

## Conflicts of interest

Professor José María Ruiz Moreno receives financial support as consultant from TOPCON. None of the remaining authors have declared any conflict of interests.

## REFERENCES

1. Fernández-Vigo JI, De-Pablo-Gómez-de-Liaño L, Fernández-Vigo C, Arcos-Villegas G, Fernández-Pérez C, García-Feijóo J, et al. Anterior chamber angle and trabecular meshwork measurements made by fourier-domain optical coherence tomography in healthy white children. J Glaucoma. 2017;26:810–5.
2. Fernández-Vigo JI, De-Pablo-Gómez-de-Liaño L, Kudsieh B, Fernández-Vigo C, Fernández-Vigo JÁ, García-Feijóo J. Anterior chamber angle tissue as an incidental optical coherence tomography finding in a large healthy caucasian child population. J Glaucoma. 2018;27:117–20.
3. Marion KM, Maram J, Pan X, Dastiridou A, Zhang Z, Ho A, et al. Reproducibility and agreement between 2 spectral domain optical coherence tomography devices for anterior chamber angle measurements. J Glaucoma. 2015;24:642–6.

4. Fernández-Vigo JI, García-Feijóo J, Martínez-de-la-Casa JM, García-Bella J, Arriola-Villalobos P, Fernández-Pérez C, et al. Fourier domain optical coherence tomography to assess the iridocorneal angle and correlation study in a large Caucasian population. BMC Ophthalmol. 2016;18:42.
5. Akil H, Dastiridou A, Marion K, Francis B, Chopra V. Repeatability, reproducibility, agreement characteristics of 2 SD-OCT devices for anterior chamber angle measurements. Can J Ophthalmol. 2017;52:166–70.
6. Xu BY, Mai DD, Penteado RC, Saunders L, Weinreb RN. Reproducibility and Agreement of Anterior Segment Parameter Measurements Obtained Using the CASIA2 and Spectralis OCT2 Optical Coherence Tomography Devices. J Glaucoma. 2017;26:974–9.
7. Sarunic M, Asrani S, Izatt J. Imaging the anterior segment with real time, full-range Fourier-domain optical coherence tomography. Arch Ophthalmol. 2008;126:537–42.
8. Quek DT, Narayanaswamy AK, Tun TA, Htoon HM, Baskaran M, Perera SA, et al. Comparison of 2 spectral domain optical coherence tomography devices for angle-closure assessment. Invest Ophthalmol Vis Sci. 2012;53:5131–6.
9. Wong HT, Lim MC, Sakata LM, Aung HT, Amerasinghe N, Friedman DS. High-definition optical coherence tomography imaging of the iridocorneal angle of the eye. Arch Ophthalmol. 2009;127:256–60.
10. Fernández-Vigo JI, García-Feijóo J, Martínez-de-la-Casa JM, García-Bella J, Fernández-Vigo JA. Morphometry of the trabecular meshwork in vivo in a healthy population using Fourier domain optical coherence tomography. Invest Ophthalmol Vis Sci. 2015;56:1782–8.
11. Tun TA, Baskaran M, Zheng C. Assessment of trabecular meshwork width using swept source optical coherence tomography. Graefes Arch Clin Exp Ophthalmol. 2013;251:1587–92.
12. Cheung CY, Zheng C, Ho CL. Novel anterior-chamber angle measurements by high-definition optical coherence tomography using the Schwalbe line as the land mark. Br J Ophthalmol. 2011;95:955–9.
13. Usui T, Tomidokoro A, Mishima K, Mataki N, Mayama C, Honda N, et al. Identification of Schlemm's Canal and Its Surrounding Tissues by Anterior Segment Fourier Domain OCT. Invest Ophthalmol Vis Sci. 2011;52:6934–9.
14. Kagemann L, Nevins JE, Jan NJ, Wollstein G, Ishikawa H, Kagemann J, et al. Characterisation of Schlemm's canal cross-sectional area. Br J Ophthalmol. 2014;98 Suppl 2:10–4.
15. Fernández-Vigo JI, Kudsieh B, De-Pablo L, Almorín Fernández-Vigo I, Fernández-Vigo C, Garcia-Feijóo J, et al. Schlemm's canal measured by optical coherence tomography and correlation study in a healthy Caucasian child population. Acta Ophthalmol. 2019;97:e493–8.
16. Chen J, Huang H, Zhang S, Chen X, Sun X. Expansion of Schlemm's canal by travoprost in healthy subjects determined by Fourier-domain optical coherence tomography. Invest Ophthalmol Vis Sci. 2013;54:1127–34.
17. Hong J, Xu J, Wei A, Wen W, Chen J, Yu X, et al. Spectral-domain optical coherence tomographic assessment of Schlemm's canal in Chinese subjects with primary open-angle glaucoma. Ophthalmology. 2013;120:709–15.
18. Imamoglu S, Sevim MS, Alpogan O, Ercalik NY, Kumral ET, Pekel G, et al. In vivo biometric evaluation of Schlemm's canal with spectral-domain optical coherence tomography in pseuduexfoliation glaucoma. Acta Ophthalmol. 2016;94:e688–92.
19. Skaat A, Rosman MS, Chien JL, Mogil RS, Ren R, Liebmann JM, et al. Effect of pilocarpine hydrochloride on the Schlemm canal in healthy eyes and eyes with open-angle glaucoma. JAMA Ophthalmol. 2016;134:976–81.
20. Zhao Z, Zhu X, He W, Jiang C, Lu Y. Schlemm's canal expansion after uncomplicated phacoemulsification surgery: an optical coherence tomography study. Invest Ophthalmol Vis Sci. 2016;57:6507–12.
21. Skaat A, Rosman MS, Chien JL, Ghassibi MP, Liebmann JM, Ritch R, et al. Microarchitecture of Schlemm canal before and after selective laser trabeculoplasty in enhanced depth imaging optical coherence tomography. J Glaucoma. 2017;26:361–6.
22. Hong J, Yang Y, Wei A, Deng SX, Kong X, Chen J, Girard MJ, Mari JM, Xu J, Sun X. Schlemm's canal expands after trabeculectomy in patients with primary angle-closure glaucoma. Invest Ophthalmol Vis Sci. 2014;55:5637–42.
23. Fuest M, Kuerten D, Koch E, Becker J, Hirsch T, Walter P, et al. Evaluation of early anatomical changes following canaloplasty with anterior segment spectral-domain optical coherence tomography and ultrasound biomicroscopy. Acta Ophthalmol. 2016;94:e287–92.
24. Huang AS, Francis BA, Weinreb RN. Structural and functional imaging of aqueous humour outflow: a review. Clin Exp Ophthalmol. 2018;46:158–68.
25. Console JW, Sakata LM, Aung T, Friedman DS, He M. Quantitative analysis of anterior segment optical coherence tomography images: the Zhongshan Angle Assessment Program. Br. J. Ophthalmol. 2008;92:1612–6.
26. Congdon NG, Spaeth GL, Augsburger J, Klancnik J, Patel K, Hunter DG. A proposed simple method for measurement in the anterior chamber angle: biometric gonioscopy. Ophthalmology. 1999;106:2161–7.
27. Rigi M, Bell NP, Lee DA, Baker LA, Chuang AZ, Nguyen D, et al. Agreement between Gonioscopic Examination and Swept Source Fourier Domain Anterior Segment Optical Coherence Tomography Imaging. J Ophthalmol. 2016;2016:1727039.
28. Tun TA, Baskaran M, Tan SS, Perera SA, Aung T, Husain R. Evaluation of the anterior segment angle-to-angle scan of cirrus high-definition optical coherence tomography and comparison with gonioscopy and with the visante OCT. Invest Ophthalmol Vis Sci. 2017;58:59–64.
29. Lavanya R, Foster PJ, Sakata LM. Screening for narrow angles in the singapore population: evaluation of new noncontact screening methods. Ophthalmology. 2008;115:1720–7.
30. Sakata LM, Lavanya R, Friedman DS, Aung HT, Gao H, Kumar RS, et al. Comparison of gonioscopy and anterior segment ocular coherence tomography in detecting angle closure in different quadrants of the anterior chamber angle. Ophthalmology. 2008;115:769–74.
31. Fernández-Vigo JI, De-Pablo-Gomez-De-Liaño L, Almorín-Fernández-Vigo I, Fernández-Vigo C, Macarro-Merino A, García-Feijóo J, et al. Agreement between Pentacam and optical coherence tomography in the assessment of iridocorneal angle width in a large healthy population. J Fr Ophtalmol. 2018;41:14–20.
32. Grewal DS, Brar GS, Jain R, Grewal SP. Comparison of Scheimpflug imaging and spectral domain anterior segment optical coherence tomography for detection of narrow anterior chamber angles. Eye (Lond). 2011;25:603–11.
33. Mansouri K, Sommerhalder J, Shaarawy T. Prospective comparison of ultrasound biomicroscopy and anterior segment optical coherence tomography for evaluation of anterior chamber dimensions in European eyes with primary angle closure. Eye (Lond). 2010;24:233–9.
34. Radhakrishnan S, Goldsmith J, Huang D, Westphal V, Dueker DK, Rollins AM. Comparison of coherence tomography and ultrasound biomicroscopy for detection of narrow anterior chamber angles. Arch Ophthalmol. 2005;123:1053–9.
35. Xu L, Cao WF, Wang YX, Chen CX, Jonas JB. Anterior chamber depth and chamber angle and their associations with ocular

and general parameters: the Beijing Eye Study. Am J Ophthalmol. 2008;145:929–36.
36. Pavlin CJ, Harasiewicz K, Foster FS. Ultrasound biomicroscopy of anterior segment in normal and glaucomatous eys. Am J Ophthalmol. 1992;113:381–9.
37. Leung CKS, Li H, Weinreb RN, Liu J, Cheung CY, Lai RY. Anterior Chamber Angle Measurement with Anterior Segment Optical Coherence Tomography: A Comparison between SlitLamp OCT and Visante OCT. Invest Ophthalmol Vis Sci. 2008;49:3469–74.
38. Wirbelauer C, Karandish A, Haberle H, Pham D. Non-contact goniometry with optical coherence tomography. Arch Ophthalmol. 2005;123:179–85.
39. Baskaran M, Ho SW, Tun TA, How AC, Perera SA, Friedman DS, et al. Assessment of circumferential angle-closure by the iris-trabecular contact index with swept-source optical coherence tomography. Ophthalmology. 2013;120:2226–31.
40. Fernández-Vigo JI, De-Pablo-Gomez-De-Liaño L, Fernández-Vigo C, Sánchez-Guillén I, Santos-Bueso E, Martínez-de-la-Casa JM, et al. Quantification of trabecular-iris contact and its prevalence by optical coherence tomography in a healthy Caucasian population. Eur J Ophthalmol. 2017;27:417–22.
41. Chong RS, Sakata LM, Narayanaswamy AK, Ho SW, He M, Baskaran M, et al. Relationship between intraocular pressure and angle configuration: an anterior segment OCT study. Invest Ophthalmol Vis Sci. 2013;54:1650–5.
42. Shabana N, Aquino MC, See J, Ce Z, Tan AM, Nolan WP, et al. Quantitative evaluation of anterior chamber parameters using anterior segment optical coherence tomography in primary angle closure mechanisms. Clin Exp Ophthalmol. 2012;40:792–801.
43. Guzman CP, Gong T, Nongpiur ME, Perera SA, How AC, Lee HK, et al. Anterior segment optical coherence tomography parameters in subtypes of primary angle closure. Invest Ophthalmol Vis Sci. 2013;54:5281–6.
44. Kwon J, Sung KR, Han S, Moon YJ, Shin JW. Subclassification of primary angle closure using anterior segment optical coherence tomography and ultrasound biomicroscopic parameters. Ophthalmology. 2017;124:1039–47.
45. Wirbelauer C, Karandish A, Häberle H, Pham DT. Optical coherence tomography in malignant glaucoma following filtration surgery. Br J Ophthalmol. 2003;87:952–5.
46. Sugimoto Y, Mochizuki H, Okumichi H, Takumida M, Takamatsu M, Kawamata S, et al. Effect of intravitreal bevacizumab on iris vessels in neovascular glaucoma patients. Graefes Arch Clin Exp Ophthalmol. 2010;248:1601–9.
47. Nadal J, Carreras E, Kudsieh B, Canut M. Neovascular glaucoma treatment with extraction of anterior chamber fibrovascular tissue. JAMAOphthalmol. 2013;131:1083–5.
48. Birner B, Tourtas T, Wessel JM, Jünemann AG, Mardin CY, Kruse FE, et al. Pigment dispersion syndrome and pigmentary glaucoma. Morphometric analysis of the anteriorchamber segment with SL-OCT. Ophthalmologe. 2014;111:638–43.
49. Aptel F, Beccat S, Fortoul V, Denis P. Biometric analysis of pigment dispersion syndrome using anterior segment optical coherence tomography. Ophthalmology. 2011;118:1563–70.
50. Fernández-Vigo JI, De-Pablo-Gomez-De-Liaño L, Sánchez-Guillen I, Macarro-Merino A, Fernández-Vigo C, García-Feijóo J, et al. Pseudoexfoliation signs in the anterior segment assessed by optical coherence tomography and Scheimpflug device. Arch Soc Esp Oftalmol. 2018;93:53–9.
51. Moghimi S, Chen R, Johari M. Changes in anterior segment morphology after laser peripheral iridotomy in acute primary angle closure. Am J Ophthalmol. 2016;166:133–40.
52. Yoong Leong JC, O'Connor J, Soon Ang G, Wells AP. Anterior segment optical coherence tomography changes to the anterior chamber angle in the short-term following laser peripheral iridoplasty. J Curr Glaucoma Pract. 2014;8:1–6.
53. Lee RY, Kasuga T, Cui QN, Huang G, He M, Lin SC. Association between baseline angle width and induced angle opening following prophylactic laser peripheral iridotomy. Invest Ophthalmol Vis Sci. 2013;54:3763–70.
54. Sung KR, Lee KS, Hong JW. Baseline anterior segment parameters associated with the long-term outcome of laser peripheral iridotomy. Curr Eye Res. 2015;40:1128–33.
55. Ang GS, Wells AP. Factors influencing laser peripheral iridotomy outcomes in white eyes: an anterior segment optical coherence tomography study. J Glaucoma. 2011;20:577–83.
56. Zhou AW, Giroux J, Mao AJ, Hutnik CM. Can preoperative anterior chamber angle width predict magnitude of intraocular pressure change after cataract surgery? Can J Ophthalmol. 2010;45:149–53.
57. Huang G, Gonzalez E, Lee R, Chen YC, He M, Lin SC. Association of biometric factors with anterior chamber angle widening and intraocular pressure reduction after uneventful phacoemulsification for cataract. J Cataract Refract Surg. 2012;38:108–16.
58. Hsia YC, Moghimi S, Coh P, Chen R, Masis M, Lin SC. Anterior segment parameters as predictors of intraocular pressure reduction after phacoemulsification in eyes with open-angle glaucoma. J Cataract Refract Surg. 2017;43:879–85.
59. Fernández-Vigo JI, Macarro-Merino A, Fernández-Vigo C, Fernández-Vigo JA, Martínez de la Casa JM, Fernández-Pérez C, et al. Effects of Implantable Collamer Lens V4c placement on iridocorneal angle measurements by Fourier domain optical coherence tomography. Am J Ophthalmol. 2016;162:43–52.
60. Fernández-Vigo JI, Macarro-Merino A, Fernández-Vigo C, Fernández-Vigo JÁ, De-Pablo-Gomez-De-Liaño L, Fernández-Pérez C, et al. Impacts of Implantable Collamer Lens V4c Placement on Angle Measurements Made by Optical Coherence Tomography: Two-Year Follow-up. Am J Ophthalmol. 2017;181:37–45.
61. Yan Z, Miao H, Zhao F, Wang X, Chen X, Li M, et al. Two-year outcomes of visian implantable collamer lens with a central hole for correcting high myopia. J Ophthalmol. 2018;2018:8678352.